

# Unveiling the Changes in the Molecular Groups of Tight Sandstones in Response to an Electric Field

Wentong Zhang,\* Zhengfu Ning,\* Lei Song, Jie Zhu, Zongke Liu, and Hengli Wang

Cite This: *ACS Omega* 2021, 6, 29126–29136

Read Online

ACCESS |



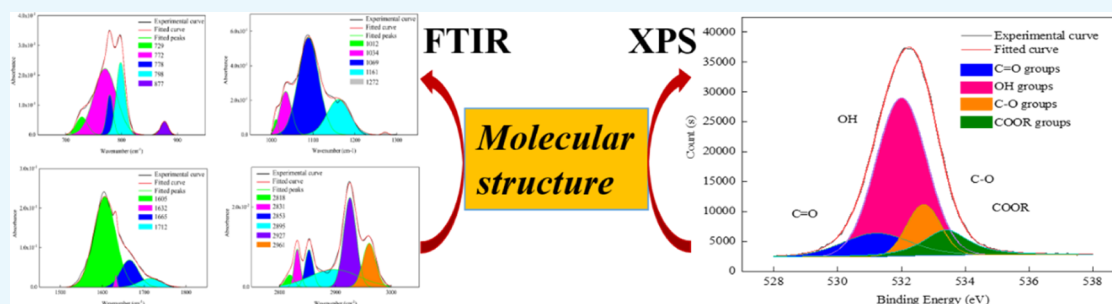
Metrics &amp; More



Article Recommendations



Supporting Information



**ABSTRACT:** The electric field method proved in the lab and oil fields is an effective and fast way to significantly improve oil recovery, which can be applied to greatly realize the urgent-need requirements for energy, especially in tight sandstones. Generally, the changed molecular groups treated with an electric field modulate the wettability of reservoirs, affecting the final oil recovery. Herein, the investigation of the impact of the electric field on the molecular groups of reservoirs is imperative and meaningful. In this paper, tight sandstones were placed into a particular instrument and subjected to various strengths of the electric field. Nine treated powders and one untreated powder of tight sandstones were processed by Fourier transform infrared spectroscopy (FTIR) and X-ray photoelectron spectroscopy (XPS) experiments. FTIR results show that the electric field decreases aromatic groups, C–O groups, COOH groups, and aliphatic groups, whereas it increases C=C groups, C=O groups, and OH groups. Interestingly, the changes in C–O groups, C=O groups, COOH groups, and OH groups are all the competitive results of production and consumption during the treatment process. With regard to C–O groups and COOH groups, the consumption has an advantage over the production on the content of functional groups, and the situations for C=C groups and OH groups exhibit a contrary trend. The fitted result of XPS proves the fact that the electric field improves C=O groups, OH groups, and COOR groups, whereas it reduces C–O groups, supporting that the molecular groups can be mutually transformed during the electric field treatment. The obtained knowledge is beneficial to the study of electric field-related technologies on the molecular groups of reservoirs.

## 1. INTRODUCTION

In a recent paper on science, Joon Heo puts forward a special approach to tune the chemical properties of molecules by altering the applied voltage.<sup>1</sup> This further indicates that an electric field can modulate the molecular groups of materials. Interestingly, numerous studies demonstrate that the charges are appealed and accumulated on the solid–liquid interface by applying an electric field, where the chemical reactions occur, with the result that the molecular groups of materials will be converted.<sup>2–6</sup> Thus, according to this background, the changes in the molecular groups of materials induced by an electric field have been applied to several practical applications, such as in the treatment of oil sediments,<sup>7,8</sup> comminution of break rocks,<sup>9</sup> separation of oil and water,<sup>10</sup> and usage of electro-wetting to develop superwetting materials.<sup>11</sup> The following question may come up: whether the molecular groups of reservoirs can be altered with an electric field and further to improve oil recovery? This is because the wettability of reservoirs is closely related to the molecular groups.<sup>12</sup>

Generally, the reservoirs with a high water-wet property enhance oil recovery. With the increasing demand for more oil and gas, unconventional resources have gradually received many interests from researchers and oil companies.<sup>13–15</sup> Tight sandstone is one hotspot of alternative resources after the successful development of shale, which extremely arouses desired attention.<sup>16</sup> Significant efforts and advances (pH, surfactant, ionic liquids, and nanofluids) have been applied to tight sandstones, and several satisfied fruits have been tasted. However, many substances injected in the well rarely effectively reach the whole matrix and cause an effect because the pore throat of tight sandstones ranges from the nanoscale

Received: August 11, 2021

Accepted: October 8, 2021

Published: October 22, 2021



to the microscale,<sup>17</sup> which significantly hinders the effects in the exploitation of tight sandstones. Furthermore, the challenges of hard control, long-term effect, environmental, and safety issues still remain in these methods.<sup>18</sup> Thus, a fast, in situ, and eco-friendly active control over the tight sandstones to efficiently enhance oil recovery will be a significantly welcome and urgent need.<sup>19</sup> To date, several electric field-related experiments indicate that the production of oil and gas of reservoirs can be significantly improved by an electric field,<sup>20–30</sup> pointing out that the electric field method exhibits an impressive potential application to oil fields. Therefore, research on the changes in the molecular groups of tight sandstones subjected to an electric field is necessary to lay the groundwork in establishing the theoretical knowledge to guide the development of tight sandstones with electric field-related technologies.

With respect to petroleum engineering, the wettability of reservoirs can control the flow process and determine oil–water distribution for hydrocarbon species, influencing the ultimate oil recovery.<sup>31,32</sup> According to this principle, numerous studies have tried to modulate the wettability of reservoirs to further improve oil recovery using pH, surfactant, ionic liquids, nanofluids, CO<sub>2</sub>, and so on.<sup>18</sup> Commonly, the wettability is essentially controlled by chemical and physical factors. The physical factor is related to the surface roughness of reservoirs, while the chemical factor refers to the molecular groups of reservoirs. In our previous study, we have found that the surface roughness indeed affects the wettability, whereas the molecular groups play a dominant role in determining the wettability of reservoirs.<sup>6</sup> Numerous efforts also demonstrate that the molecular groups of reservoirs affect the wettability.<sup>33–35</sup> For example, Zhou et al. (2015) demonstrated that the increase in oxygen polar functional groups improves the hydrophilic characteristic of coal dust.<sup>36</sup> Tang et al. (2016) indicated that oxygen-related functional groups enhance the hydrophilic property of coal dust.<sup>37</sup> Xia et al. (2016) presented that the improvement in the water-wet property of the lignite is due to the augmentation of oxygen-containing molecular groups.<sup>38</sup> Xu et al. (2017) showed that the increase in the hydroxyl groups exhibits a good linear relationship with the water-wet property of coal dust.<sup>39</sup> Wang et al. (2017) observed that the augmentation in the oxygen-related functional groups enhances the water-wet property of coal dust.<sup>33</sup> Thus, the molecular groups of reservoirs have a close relationship with its wettability. Usually, a high content of oxygen-containing molecular groups causes more water wetting. Furthermore, some scholars indicated that the aliphatic groups have a contrary effect on the wettability.<sup>40–43</sup> Thus, it is interesting and crucial to investigate molecular groups, which can help to evaluate the wettability of reservoirs.

As for the molecular groups, Fourier transform infrared spectroscopy (FTIR) is a quick and helpful technique to investigate the molecular groups of fossil fuels. FTIR can recognize vibrational signals to identify the functional groups on the surface of fossil fuels.<sup>44,45</sup> In addition, X-ray photoelectron spectroscopy (XPS) can analyze the chemical property and quantitatively determine the content of functional groups of fossil fuels.<sup>36,46,47</sup> Thus, FTIR and XPS have been broadly applied to reservoirs to reveal their molecular groups.<sup>34,48–50</sup> For example, Wang et al. (2017) performed FTIR to identify the molecular groups of coal dust. The results show that aromatic groups and aliphatic groups repel water, while the hydroxyl groups and carboxyl groups absorb water.<sup>33</sup>

He et al. (2017) conducted FTIR to determine the molecular groups of different-rank coals.<sup>51,52</sup> The results indicate that the growth of aromatic groups exhibits an upward graphitization. Zhao et al. (2019) applied FTIR to illustrate the changes in the molecular groups of coal subjected to high-temperature oxidation. The results show that functional groups can be consumed and reproduced in the oxidation process.<sup>53</sup> Ni et al. (2019) utilized FTIR to build a relationship between the molecular groups and the wettability of coal subjected to NaCl-SDS compound treatment. The results demonstrate that aliphatic groups impose the most significant influence on wettability, followed by aromatic hydrocarbons and oxygen-related functional groups.<sup>40–43</sup> Wang et al. (2017) applied XPS to investigate the molecular groups of lignite. The results indicate that the oxygen-related functional groups of coal exhibit a style of side chains and crosslinking.<sup>54</sup> Liu et al. (2019) united FTIR and XPS to compare the molecular groups of hard and soft coal. The results present that the increases in aromatic groups and aliphatic hydrocarbons with reductions in C=O groups and OH groups improve the maturity of hard coals.<sup>55</sup> Zhang et al. (2017) combined FTIR and XPS to study the molecular groups of low-rank coal treated by microwave-assisted heating. The results imply that C–O groups occupy a dominant percentage in the oxygen-related groups.<sup>56</sup>

As reported, FTIR and XPS can be applied to reveal the information about the molecular groups of fossil fuels. Taking the potential application of the electric field in tight sandstones into consideration, investigating the changes in the molecular groups induced by an electric field enables a thorough understanding of the role of the electric field in the tight sandstones. Despite the fact that efforts on the relationship between oxygen-related functional groups and the wettability of tight sandstones treated with an electric field have been reported in our previous study,<sup>6</sup> several unresolved issues still remain. For example, in our previous publication, the main attention is given to build a relationship between oxygen-related functional groups and the wettability of tight sandstones treated with an electric field. The changes in the other molecular groups (aromatic rings, hydrocarbon compounds, and C=C groups) are still unclear. Meanwhile, the mechanism in the alterations for these molecular groups is still obscure. Thus, this paper aims to reveal the changes in the molecular groups of tight sandstones in response to an electric field, which provides a facile route for developing tight sandstones and induces people eager to improve the success in applying electric field-related technologies on tight sandstones. Notably, the role of the molecular groups in the wettability can be referred to in our previous publication. In this study, we try to reveal the mechanism of variations in the molecular groups.

To investigate the changes in the molecular groups of the reservoirs triggered by an electric field, four tight sandstones were placed into a particular core holder and subjected to various strengths of the electric field. Nine treated powders from three different treated regions (anode, middle, and cathode) and one untreated powder were processed by FTIR and XPS experiments. After that, the information about the changes in the molecular groups of tight sandstones treated with an electric field will be revealed through the combined analysis of FTIR and XPS.

## 2. RESULTS

**2.1. Results of FTIR.** A total of 10 FTIR spectra are shown in Figure 1. Region I presents the vibration of aromatic groups

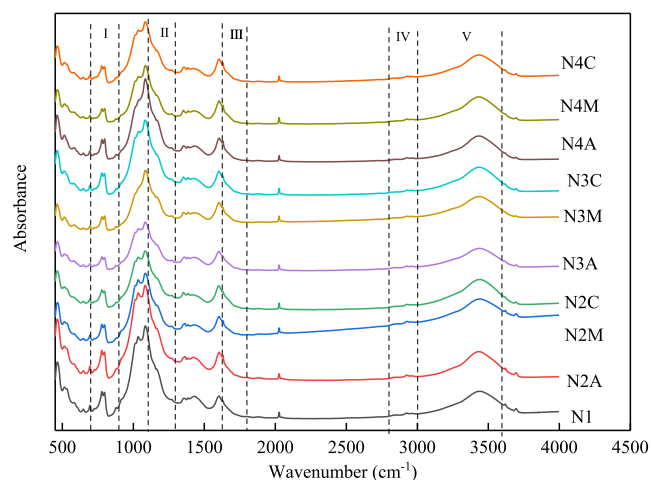


Figure 1. Total of 10 FTIR spectra.

(700–900  $\text{cm}^{-1}$ );<sup>56</sup> correspondingly, the fitted results for the bond region of aromatic groups are indicated in Figure 2a. Region II shows the vibration of alcohol and ether (1100–1300  $\text{cm}^{-1}$ ),<sup>40,43</sup> and region III indicates the vibration of the skeleton of C=C and carbonyl groups.<sup>44,57</sup> Region II and region III are attributed to the vibration of the oxygen-containing structure.<sup>58</sup> The fitted results of two regions are

shown in Figure 2b,c, respectively. Region IV demonstrates the vibration of aliphatic groups (2800–3000  $\text{cm}^{-1}$ ),<sup>43,59</sup> and the fitted results of region IV are depicted in Figure 2d. Region V belongs to the vibration of the hydroxyl group (3000–3600  $\text{cm}^{-1}$ ). More detailed information about the molecular groups of tight sandstones will be discussed in the following sections.

**2.1.1. Variations in Aromatic Groups.** As for the aromatic groups in Figure 2a, the peak of 729  $\text{cm}^{-1}$  is the vibration of monosubstituted benzene, the peaks of 772 and 778  $\text{cm}^{-1}$  belong to the vibration of 1,2-disubstituted benzene, the peak of 798  $\text{cm}^{-1}$  presents the vibration of 1,3-disubstituted benzene, and the peak of 877  $\text{cm}^{-1}$  means the vibration of 1,4-disubstituted benzene based on the study of Ni.<sup>43</sup> After that, based on the definition of the area ratio, the area ratios of various kinds of aromatic groups (700–900  $\text{cm}^{-1}$ ) are shown in Figure 3a, and the area ratio of total aromatic groups is indicated in Figure 3b. Figure 3a,b implies that the area ratios of different kinds of aromatic groups and total aromatic groups in treated samples are all below 1.0 when tight sandstones were treated by different strengths of electric field, showing that the electric field drops aromatic groups. Moreover, it is found that there is an inconsistent downward trend with the increasing strengths of the electric field in Figure 3a,b, which indicates that although the impact of locations still remains, the effect of the electric field is obviously stronger than the role of locations. Thus, the analysis of the changes in the molecular groups of tight sandstones subjected to an electric field can be reliable.

Ferric ions ( $\text{Fe}^{3+}$ ) are produced in the anode region (eqs 1–3), passed by the middle region, and concentrated in the cathode region with the role of an external electric field (this

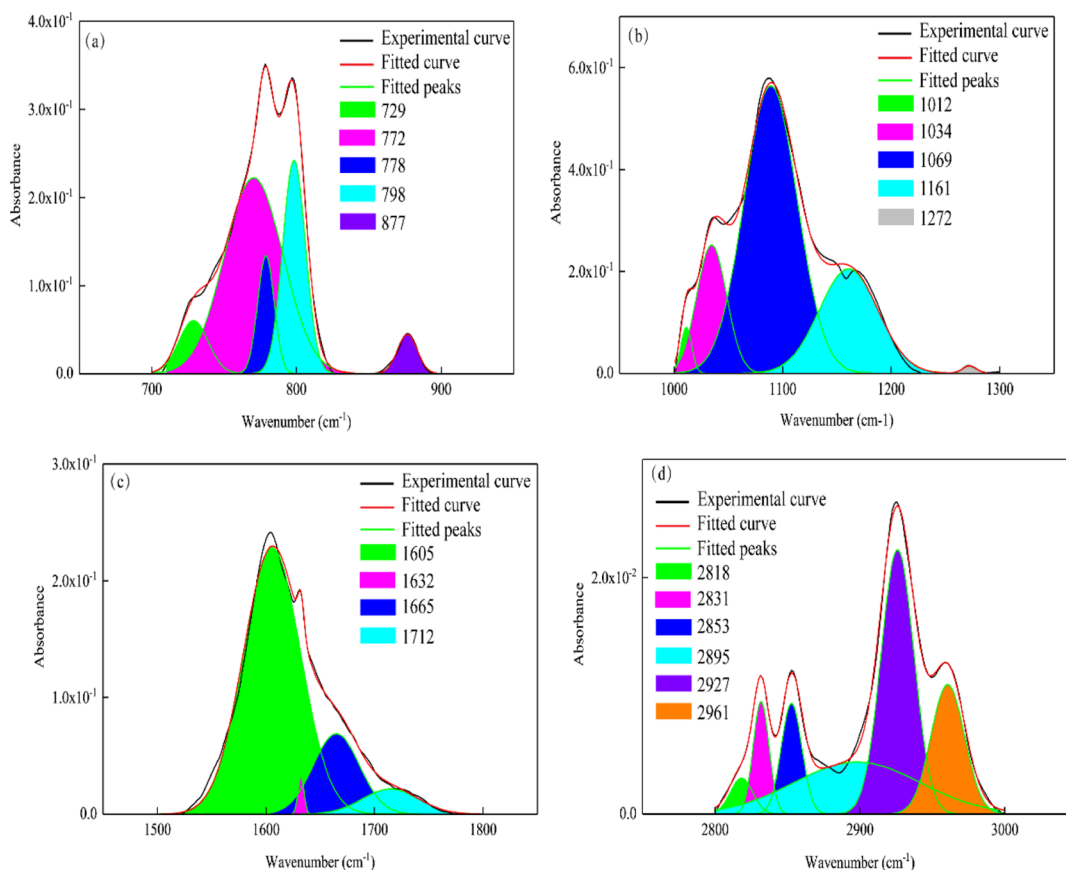
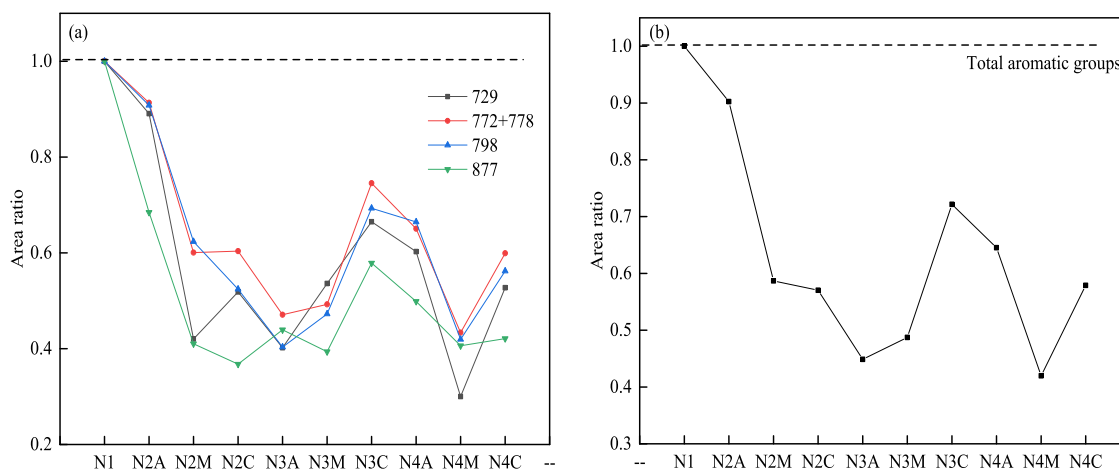
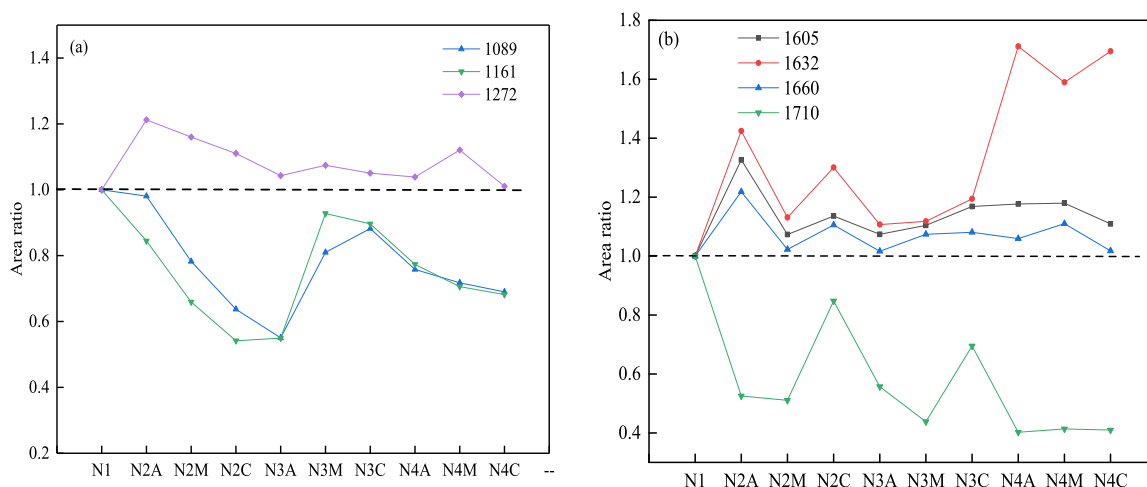


Figure 2. Fitted results for different bond regions. (a) 700–900; (b) 1000–1300; (c) 1500–1800; and (d) 2800–3000  $\text{cm}^{-1}$ .



**Figure 3.** Results of aromatic groups, (a) different kinds of aromatic groups and (b) total aromatic groups.

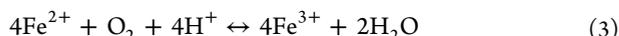


**Figure 4.** Results of fitted molecular groups, (a) C–O groups and (b) C=C and C=O groups.

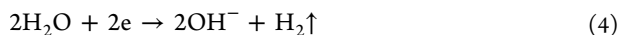
can be proved by the contents of iron elements of XPS, which is shown in the Supporting Information.<sup>60</sup> With respect to the cathode region (eq 4), the impact of the oxidation effect of ferric ions is usually higher than the effect of the reduction of hydroxide ions.<sup>6</sup> Thus, the oxidation reaction happens in three treated regions (anode, middle, and cathode regions) in the existence of the electric field.

Under the influence of the oxidation effect, the evaporation of some small molecules with aromatic groups and the loss of several aromatic fragments shed from C–O exhibit a downward trend for aromatic groups.<sup>46,53</sup> Moreover, the ring of benzene may be cracked in the participation of the electric field.<sup>61</sup> Thus, the content of aromatic groups exhibits a declining tendency under the impact of the electric field.

Anode region



Cathode region



**2.1.2. Changes in C–O, C=O, and C=C Groups.** As seen in Figure 2b, the peak of 1089  $\text{cm}^{-1}$  means the vibration of C–

O–C groups,<sup>45</sup> the peak of 1161  $\text{cm}^{-1}$  belongs to the vibration of C–O groups, and the peak of 1272  $\text{cm}^{-1}$  is attributed to the vibration of hydroxybenzene (Ar–OH) groups.<sup>45,62,63</sup> The fitted results of C–O–C groups, C–O groups, and Ar–OH are presented in Figure 4a. Figure 4a shows that the area ratios of C–O–C groups and C–O groups in treated samples are below 1.0 with the effect of an electric field, which demonstrates that the electric field reduces the contents of C–O–C groups and C–O groups. On the contrary, the area ratio of Ar–OH groups in treated samples exceeds 1.0 with the presence of an electric field, which means that the electric field improves the amounts of Ar–OH groups.

In terms of the molecular groups in Figure 2c, the peak of 1605  $\text{cm}^{-1}$  means the vibration of C=C groups, the peaks of 1632 and 1660  $\text{cm}^{-1}$  belong to the vibration of C=O groups, and the peak of 1710  $\text{cm}^{-1}$  is regarded as the vibration of COOH groups.<sup>44,57</sup> The area ratios of C=C groups, C=O groups, and COOH groups are depicted in Figure 4b. Figure 4b demonstrates that the area ratios of C=C groups and C=O groups surpass 1.0 with the role of an electric field, which indicates that the electric field enhances the numbers of C=C groups and C=O groups. Correspondingly, the descending trend in the area ratio of COOH groups in Figure 4b points out that the electric field degrades COOH groups.

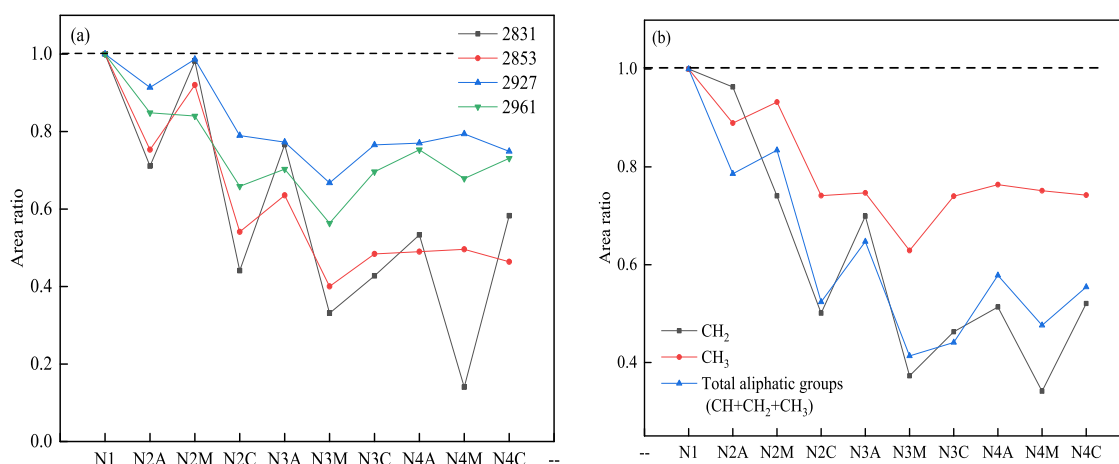


**Figure 5.** Results of aliphatic groups, (a) symmetrical and asymmetrical CH<sub>2</sub> and CH<sub>3</sub> groups and (b) CH<sub>2</sub>, CH<sub>3</sub>, and total aliphatic groups.

**2.1.3. Evolutions in CH<sub>2</sub> and CH<sub>3</sub> Groups.** As is shown in Figure 2d, there appear six individual peaks for the vibrations of CH groups, CH<sub>2</sub> groups, and CH<sub>3</sub> groups.<sup>59</sup> Concretely, the peaks of 2818 and 2895 cm<sup>-1</sup> are classified as the vibration of CH groups, the peaks of 2831 and 2925 cm<sup>-1</sup> belong to the vibration of symmetrical CH<sub>2</sub> groups and asymmetrical CH<sub>2</sub> groups, respectively, and the peaks of 2853 and 2961 cm<sup>-1</sup> are attributed to the vibration of symmetrical CH<sub>3</sub> groups and asymmetrical CH<sub>3</sub> groups, respectively.<sup>59</sup> The area ratios of CH<sub>2</sub> groups and CH<sub>3</sub> groups are presented in Figure 5a, and the area ratio of the total aliphatic groups (CH + CH<sub>2</sub> + CH<sub>3</sub>) is shown in Figure 5b.

Figure 5a shows that the area ratios of CH<sub>2</sub> groups and CH<sub>3</sub> groups in treated samples are below 1.0 with an applied electric field, indicating that the electric field weakens the contents of CH<sub>2</sub> groups and CH<sub>3</sub> groups. It is also noticed that the downward span of CH<sub>2</sub> groups is higher than that of CH<sub>3</sub> groups in Figure 5b. This demonstrates that CH<sub>2</sub> groups take more part in the chemical action than the participation of CH<sub>3</sub> groups under the role of the electric field, with the result that the consumption of CH<sub>2</sub> groups is higher than that of CH<sub>3</sub> groups. This observation corresponds to the conclusions of Zhao.<sup>53</sup> Furthermore, the trend of CH<sub>2</sub> groups keeps a good agreement with that of the total aliphatic groups (CH + CH<sub>2</sub> + CH<sub>3</sub>) in Figure 5b, indicating that CH<sub>2</sub> groups occupy a dominant percentage in the amount of total aliphatic groups.

**2.1.4. Alteration in OH Groups.** The area ratios of hydroxyl groups in the bond region of 3000–3600 cm<sup>-1</sup> and the total hydroxyl groups [(3000 – 3600) + 1272] are shown in Figure 6. It is found that the area ratio of hydroxyl groups (3000–3600 cm<sup>-1</sup>) of the N3A sample is less than 1.0, while the area ratio of the total hydroxyl groups [(3000 – 3600) + 1272] of the N3A exceeds 1.0. To sum up, the area ratios in the total hydroxyl groups in treated samples in Figure 6 are all larger than 1.0 under the effect of the electric field, indicating that the electric field increases the numbers of OH groups. (The results of XPS can also prove it, which will be discussed later.)

**2.2. Comparisons between FTIR and XPS.** Usually, the binding energy of the oxygen element ranges from 528 to 538 eV. The obtained XPS curves of the oxygen element are shown in Figure 7a. Figure 7a indicates that the amounts of oxygen element are assuredly tuned under the influence of an electric field. The contents of the oxygen element for treated samples (N2, N3, and N4) are obviously higher than those of the untreated sample (N1), demonstrating that the electric field

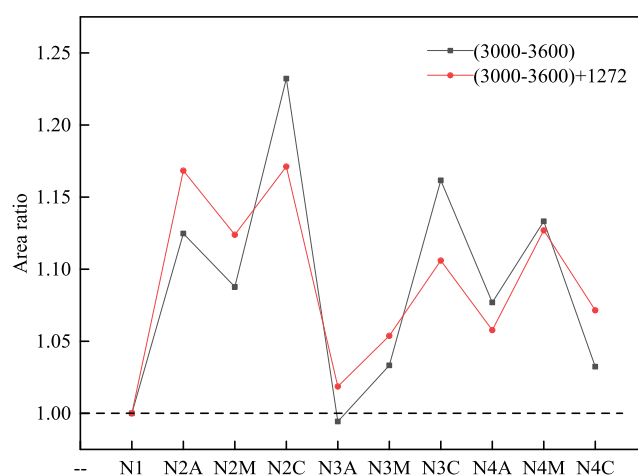


**Figure 6.** Results of hydroxyl groups.

augments the quantity of oxygen element in tight sandstones. In order to quantitatively refine the contents of various oxygen-related functional groups, the oxygen element (O 1s) of 10 powders is peak-differentiated and imitated based on the rule that the binding energies for various kinds of oxygen-related functional groups (C=O, OH, C–O, and COOR) are 531.2, 532, 532.7, and 533.4 eV, respectively.<sup>54,55</sup> This fitting process is depicted in Figure 7b.

The area ratios of various kinds of molecular groups calculated through XPS are displayed in Figure 8. Comparably, the area ratios of the corresponding molecular groups determined by FTIR are also presented in Figure 8 to assess the fitted results of FTIR.

With respect to the fitted results of XPS, it is found that the area ratios of C=O groups, OH groups, and COOR groups for treated samples all exceed 1.0 under the role of the electric field, showing that the electric field raises the contents of C=O groups, OH groups, and COOR groups. Furthermore, the area ratios of C–O groups for treated samples are less than 1.0 under the effect of an electric field, meaning that the electric field reduces the numbers of C–O groups. It is noticed that the altered trends in C=O groups, OH groups, C–O groups, and COOR groups of XPS in Figure 8 nearly remain in good accordance with those of FTIR, which supports the aforementioned analysis from FTIR results.

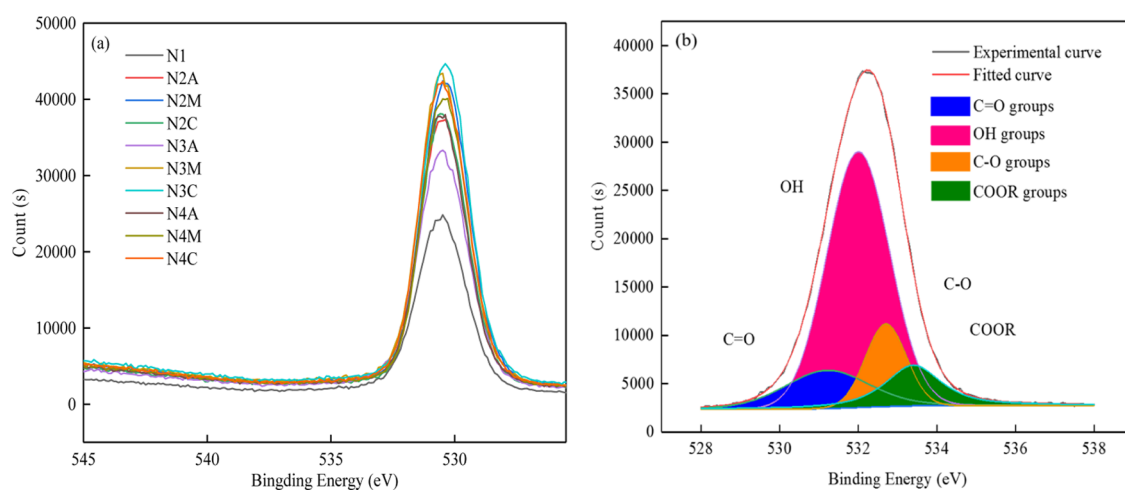


**Figure 7.** O 1s curves of XPS, (a) results of 10 samples and (b) results of fitted curves.

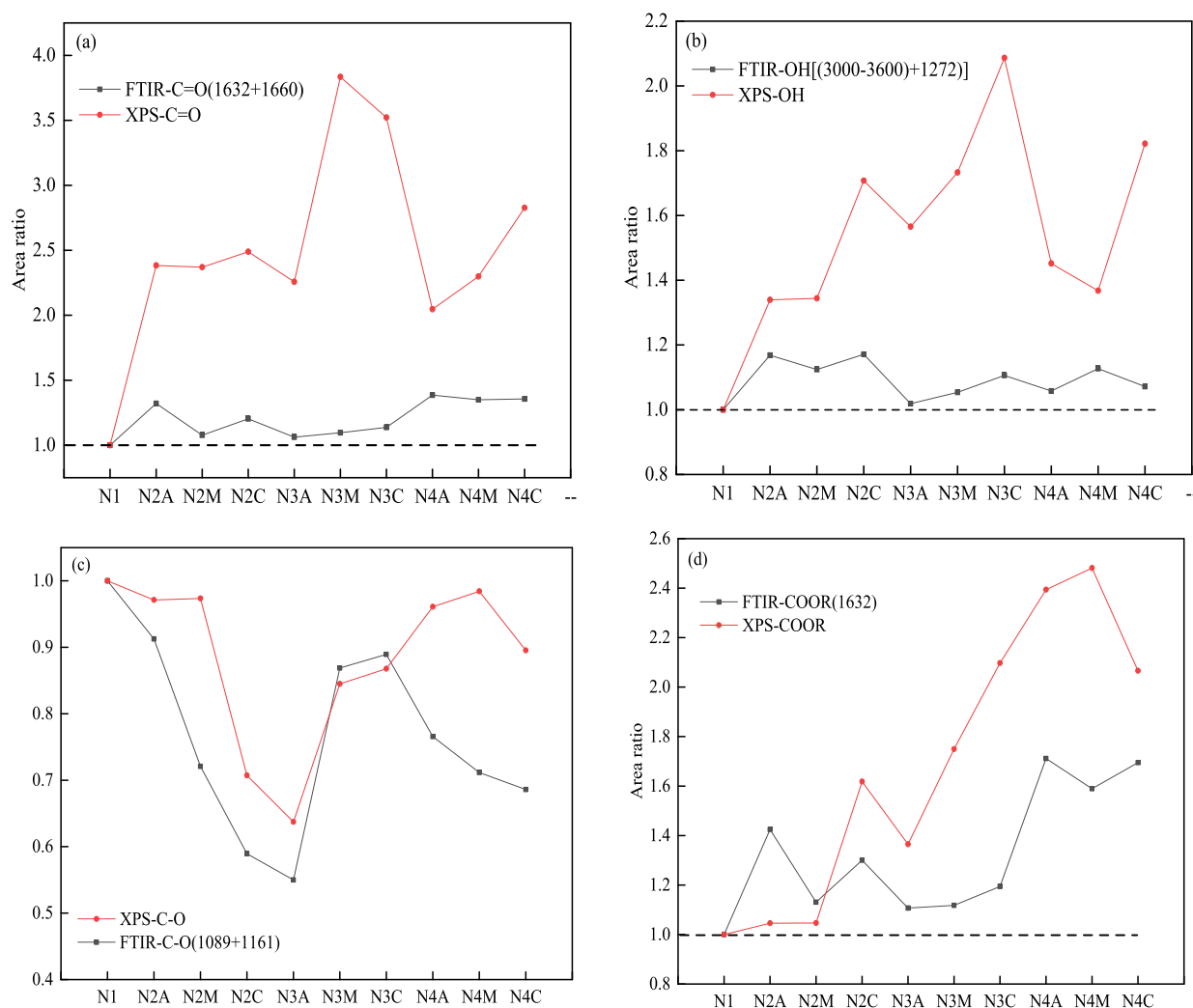


**Figure 8.** Comparisons of molecular groups between FTIR and XPS. (a) C=O groups; (b) OH groups; (c) C–O group; and (d) COOR groups.

### 3. DISCUSSION

Current would be produced in the existence of an ionic solution when an electric field is applied. Thus, the current occurs once tight sandstones filled with brine water are subjected to an electric field. After that, electrochemical actions also come into being inside the tight sandstones. The required

element in electrochemistry action is the shift of electrons. The movement of electrons causes the alteration of the electron cloud, which can break the old chemical bonds. In the meanwhile, new chemical bonds are generated. As is presented in FTIR, no new peak has come into being, indicating that the electric field induces mutual transformation between molecular

groups. As is stated, the mechanism of chemical reaction of tight sandstones treated with an electric field is the oxidation reaction because of the movement of ferric ions. Thus, the oxidation effect causes changes in the molecular groups of tight sandstones treated with an electric field. From the analysis of the previous results, FTIR and XPS all support that the electric field decreases aromatic groups, C–O groups, and aliphatic groups, whereas it increases C=C groups, C=O groups, and OH groups. Here, we discuss the potential mechanisms for alterations in these molecular groups.

With regard to oxygen-containing molecular groups (C–O, C=O, COOR, and COOH), the oxidation effect attacks the bridge bond and side chains of the aliphatic hydrocarbon, inducing more methyl and methylene groups (CH<sub>2</sub> and CH<sub>3</sub>) to be produced.<sup>53</sup> Afterward, the methyl and methylene groups are further transferred to C–O groups by an oxygen substitution (eqs 5 and 6),<sup>53,64–66</sup> which improves the content of C–O groups. Accordingly, the aliphatic groups exhibit a descending trend. However, C–O groups can also be converted to C=O groups in the participation of the oxidation effect (eq 7),<sup>38,53,66,67</sup> which somewhat consumes C–O groups. Furthermore, several molecules with fragments derived from the decomposition of C–O evaporate, consuming the amounts of C–O groups. Obviously, there exists a controversy where production and consumption occur. Thus, the changes in C–O groups are determined by the competitive results of production and consumption (CRPC). The declining trend of the area ratio of C–O groups in Figure 4a indicates that the consumption has an advantage over the role of production on the molecular groups under the electric field conditions.

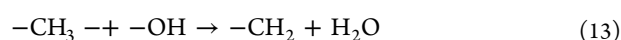
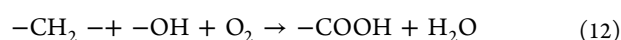
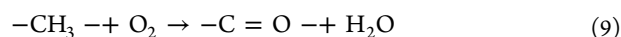
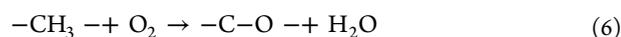
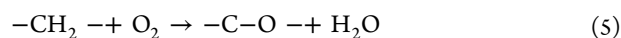
With regard to the alteration in C=O groups, apart from the conversion from C–O groups (eq 6), according to the view of Zhao, the methyl and methylene groups (CH<sub>2</sub> and CH<sub>3</sub>) are transferred to C=O groups under the oxidation effect (eqs 8 and 9).<sup>53</sup> It is noticed that eqs 8 and 9 can be derived by combing eqs 5–7. Thus, it is speculated that the aliphatic groups (CH<sub>2</sub> and CH<sub>3</sub>) first transfer to C–O groups and then convert to C=O groups under the oxidized circumstances. In addition, C=O groups can be altered to COOH groups with the help of the oxidation effect,<sup>68</sup> which consumes the numbers of C=O groups (eq 10). Thus, C=O groups are also obtained by the CRPC. The rising trend in the area ratio of C=O groups in Figure 4b indicates that the production has an advantage over the impact of consumption on the molecular groups with the applied electric field.

The COOH groups can take action with OH groups to further produce COOR groups (eq 11),<sup>69</sup> which rather improves the content of COOR groups and reduces the amount of COOH groups.<sup>53</sup> It is worth noting that the ascending trend of 1632 cm<sup>-1</sup> is contrary to the descending trend of 1710 cm<sup>-1</sup>. Considering the potential reaction in eq 11, we speculate that the peak of 1632 cm<sup>-1</sup> presents the vibration of COOR groups. As is stated, COOH groups may also be improved through the conversion from C=O groups (eq 10). Thus, the scenario of COOH groups is the same as that of other oxygen-containing molecular groups discussed above. The area ratio of COOH groups below 1.0 in Figure 4b indicates that the consumption of COOH groups has a larger effect than the production on the molecular groups under the role of an electric field. Furthermore, according to our analysis, COOR groups would be augmented, which is also proved by XPS results.

Interestingly, oxygen gas absorbed on the active sites of the surface engenders hydroxyl species, which further improves the content of hydroxyl groups (OH) with further transformation.<sup>69</sup> For example, taking Ar–OH groups into consideration, the area ratio of 1272 cm<sup>-1</sup> in treated samples exceeds 1.0 under the effect of an electric field, which indicates that the electric field increases the amounts of Ar–OH groups. This is because the peroxide from the penetration of oxygen gas reacts with carbon-free radicals to produce the hydroxyl groups, which greatly enhances the numbers of Ar–OH groups.<sup>61,70</sup> In the meanwhile, OH groups would also be consumed due to several chemical actions (eqs 10–13). Thus, the amounts of OH groups will be controlled by the CRPC. The rising trend of OH groups in Figure 6 indicates that the production in OH groups has an advantage over the consumption on their contents of functional groups under the influence of an electric field.

To sum up, the amounts of C–O groups, C=O groups, COOH, and OH groups are all the CRPC, with the results that the electric field reduces the amounts of C–O groups and COOH groups and improves the number of C=O groups at the same time.

In terms of C=C groups, the area ratio of 1605 cm<sup>-1</sup> exceeds 1.0 with the existence of an electric field, which means that the electric field improves the contents of C=C groups. As to the reason, on the one hand, C–C groups will be cracked and reconstructed to C=C groups under the oxidation effect conditions, enhancing the amounts of C=C groups. Meanwhile, the C=C groups may also be produced from the dehydrogenation of naphthenic groups.<sup>38,66,67</sup> This induces a declining trend for C=C groups. As to the reason behind the fact that the CH<sub>2</sub> groups and CH<sub>3</sub> groups show a downward trend with the effect of an electric field, a large amount of CH<sub>3</sub> groups and CH<sub>2</sub> groups can be evaporated through the cleavage form side chains of aliphatic hydrocarbons and bridge bonds as a result of the oxidation effect.<sup>53</sup> Meanwhile, more CH<sub>3</sub> groups and CH<sub>2</sub> groups are altered to the oxygen-related molecular groups (C=O groups, C–O groups, and COOH groups) under the action of oxygen substitution.<sup>68</sup> Moreover, the hydroxyl groups react with the CH<sub>3</sub> groups and CH<sub>2</sub> groups to further produce the COOH groups (eqs 11 and 12),<sup>53,67</sup> which also consumes the amounts of aliphatic groups. Thus, C=C groups and aliphatic groups would be reduced under the influence of the electric field.



#### 4. CONCLUSIONS

To investigate the changes in the molecular groups of tight sandstones under the action of an electric field, four tight

sandstone samples were treated by various strengths of electric field. Nine treated powders and one untreated powder were processed by FTIR and XPS experiments. From the detailed analysis of FTIR and XPS, several conclusions can be drawn. In light of FTIR, the electric field decreases the contents of aromatic groups and aliphatic groups. Furthermore, the electric field reduces the content of C–O groups and improves the numbers of C=C groups, C=O groups, and OH groups. Moreover, no new peak occurs in FTIR spectra, indicating that the molecular groups can be interactively transformed under the electric field conditions. It is found that the evolutions of C–O groups, C=O groups, COOH groups, and OH groups are all the CRPC. With regard to C–O groups and COOH groups, the consumption has an advantage over the production of the molecular groups. However, with respect to C=O groups and OH groups, the production has an advantage over the consumption of their molecular groups. With regard to XPS, XPS results show that the electric field improves the contents of C=O groups, OH groups, and COOR groups, while it reduces the numbers of C–O groups. The fitted results of XPS keep a good agreement with the FTIR results, which further supports the conclusions drawn from FTIR.

## 5. EXPERIMENTS

**5.1. Materials.** Tight sandstone samples treated with an electric field always are in the form of a cylinder, while the standard samples detected by FTIR and XPS are all powders. Thus, challenges remain in the comparison of the same sample before and after undergoing the effect of an electric field. Cautions need to be exerted when comparing the molecular groups of tight sandstones before and after treating with an electric field. Therefore, in order to weaken the impact of anisotropy of reservoirs, four tight sandstones are cut from the same outcrop, which is located in the Upper Triassic Yanchang Formation, Ordos Basin of China. The chemical property can be regarded as identical due to samples neighboring each other. Four various strengths of electric field (0, 5, 10, and 15 V) were used, and the experimental conduction time remains as 24 h. Different chemical effects occur in the anode region and the cathode region when an electric field is applied.<sup>60,71</sup> Thus, nine treated slices (alphabets “A”, “M”, and “C”) cut from different regions (anode, middle, and cathode) were acquired according to their location, respectively. Afterward, nine treated powders and one untreated powder crushed from these 10 slices were prepared to further be processed by FTIR and XPS experiments. Detailed information about the geological setting, these ten powders, experimental setup, and experimental process can be referred to in our previous publication.<sup>6,72</sup>

It is noticed that although the impact of anisotropy of reservoirs has been weakened because the four tight sandstones are obtained from the same outcrop, the differences in the content of molecular groups originating from the locations of the slices under various strengths of the electric field are also worried about. Thus, in this paper, the role of various strengths of the electric field in tight sandstones from different treated regions (anode, middle, and cathode) will not be discussed. Only the differences in the molecular groups between the untreated sample (N1) and the treated samples stimulated with an electric field (N2, N3, and N4) were highlighted and discussed because of the same functions.

**5.2. Experimental Methods.** FTIR experiments: 200-mesh powders prepared from the previous nine treated slices

stimulated with an electric field and one untreated slice were crushed using an agate mortar. The mixture (0.5 mg powdered samples and 120 mg of KBr) was then compressed into a transparent sheet, which was further placed into an instrument named as MAGNA-IR 560 E.S.P. The spectra were obtained in a spectrum range of 400–4000  $\text{cm}^{-1}$  at 4  $\text{cm}^{-1}$  resolution.

XPS experiments: The transparent sheets compressed from 10 powdered samples were processed through an X-ray000 300  $\mu\text{m}$ -FG ON. The Al K alpha acted as the source gun type, and the CAE pass energy in the analyzer mode is 200.0 eV. The energy step size is 1.000 eV, and the number of energy steps is 1261.

The area of a specific peak usually denotes its amount of the corresponding molecular groups. However, it is somewhat difficult to determine the area of a specific peak due to a broad bond range and the superimposition of individual peaks for FTIR spectra and XPS curves.<sup>55</sup> Thus, PeakFit software for FTIR spectra and XPSPEAK41 for XPS curves are employed to quantitatively determine the areas of individual peaks through the calculation of deconvolution.<sup>55,65,67,73–75</sup> The detailed parameters (position, area, and width) can be acquired for various kinds of molecular groups. To better describe the changes in the molecular groups of tight sandstones treated with an electric field, the concept of the area ratio was employed.<sup>65</sup> The definition of the area ratio is the area of one type of molecular groups in treated samples triggered with an electric field (N2, N3, and N4 samples) divided by a base area of relevant molecular groups in the untreated sample (N1 sample).<sup>65</sup> Based on the definition of the area ratio, it can be speculated that the area ratio of one kind of molecular groups exceeding 1.0 means that the content will be improved with an induced electric field. On the contrary, the area ratio of one kind of molecular groups being below 1.0 indicates that the amount will be reduced with the applied electric field.

## ■ ASSOCIATED CONTENT

### SI Supporting Information

The Supporting Information is available free of charge at <https://pubs.acs.org/doi/10.1021/acsomega.1c04334>.

XPS peaks of 10 samples about the iron content (PDF)

## ■ AUTHOR INFORMATION

### Corresponding Authors

Wentong Zhang – State Key Laboratory of Petroleum Resources and Prospecting, China University of Petroleum, Beijing 102249, China; Department of Chemistry, Faculty of Science, University of Alberta, Edmonton, Alberta T6G2G2, Canada; [orcid.org/0000-0003-4724-0186](https://orcid.org/0000-0003-4724-0186); Email: [564723729@qq.com](mailto:564723729@qq.com), [fnms0202@gmail.com](mailto:fnms0202@gmail.com)

Zhengfu Ning – State Key Laboratory of Petroleum Resources and Prospecting, China University of Petroleum, Beijing 102249, China; Email: [nzf@cup.edu.cn](mailto:nzf@cup.edu.cn)

### Authors

Lei Song – Changqing Oilfield Company Exploration and Development Research Institute, Xi'an 710021, China

Jie Zhu – Oilfield Technical Service Company, Xinjiang Oilfield Company, PetroChina, Karamay, Xinjiang 834000, China

Zongke Liu – State Key Laboratory of Petroleum Resources and Prospecting, China University of Petroleum, Beijing 102249, China

Hengli Wang – State Key Laboratory of Petroleum Resources and Prospecting, China University of Petroleum, Beijing 102249, China

Complete contact information is available at:  
<https://pubs.acs.org/10.1021/acsomega.1c04334>

### Author Contributions

W.Z. designed and conducted experiments, drew diagrams, analyzed data, and wrote the original manuscript. Z.N. designed experiments and guided the writing of this work. L.S. and J.Z. helped with the design of these experiments. Moreover, L.S., Z.L., and H.W. helped with the operation of experiments and put forward helpful suggestions.

### Notes

The authors declare no competing financial interest.

### ACKNOWLEDGMENTS

This work was supported by the Foundation of National Science in China (no. 51974330 and 51774298). Moreover, the first author (Wentong Zhang) gives a special thanks to the China Scholarship Council (CSC) of China for supporting his studies in the University of Alberta (no. 202006440064).

### REFERENCES

- (1) Heo, J.; Ahn, H.; Won, J.; Son, J. G.; Shon, H. K.; Lee, T. G.; Han, S. W.; Baik, M.-H. Electro-inductive effect: Electrodes as functional groups with tunable electronic properties. *Science* **2020**, *370*, 214–219.
- (2) Liu, M.; Jiang, L. Switchable adhesion on liquid/solid interfaces. *Adv. Funct. Mater.* **2010**, *20*, 3753–3764.
- (3) Zhang, G.; Duan, Z.; Wang, Q.; Li, L.; Yao, W.; Liu, C. Electrical potential induced switchable wettability of super-aligned carbon nanotube films. *Appl. Surf. Sci.* **2018**, *427*, 628–635.
- (4) Zahiri, B.; Sow, P. K.; Kung, C. H.; Mérida, W. Active control over the wettability from superhydrophobic to superhydrophilic by electrochemically altering the oxidation state in a low voltage range. *Adv. Funct. Mater.* **2017**, *4*, 1700121.
- (5) Kakade, B. A. Chemical control of superhydrophobicity of carbon nanotube surfaces: droplet pinning and electrowetting behavior. *Nanoscale* **2013**, *5*, 7011–7016.
- (6) Zhang, W.; Ning, Z.; Cheng, Z.; Wang, Q.; Wu, X.; Huang, L. Experimental Investigation of the Role of DC Voltage in the Wettability Alteration in Tight Sandstones. *Langmuir* **2020**, *36*, 11985–11995.
- (7) Kariminezhad, E.; Elektorowicz, M. Comparison of constant, pulsed, incremental and decremental direct current applications on solid-liquid phase separation in oil sediments. *J. Hazard. Mater.* **2018**, *358*, 475–483.
- (8) Kariminezhad, E.; Elektorowicz, M. Effect of various electrokinetic treatment regimes on solids surface properties and thermal behavior of oil sediments. *J. Hazard. Mater.* **2018**, *353*, 227–235.
- (9) Zuo, W.; Shi, F.; Manlapig, E. Electrical breakdown channel locality in high voltage pulse breakage. *Miner. Eng.* **2014**, *69*, 196–204.
- (10) Kung, C. H.; Zahiri, B.; Sow, P. K.; Mérida, W. On-demand oil-water separation via low-voltage wettability switching of core-shell structures on copper substrates. *Appl. Surf. Sci.* **2018**, *444*, 15–27.
- (11) Kakade, B.; Mehta, R.; Durge, A.; Kulkarni, S.; Pillai, V. Electric field induced, superhydrophobic to superhydrophilic switching in multiwalled carbon nanotube papers. *Nano Lett.* **2008**, *8*, 2693–2696.
- (12) Jia, Z.; Ning, Z.; Gao, X.; Wang, Q.; Zhang, W.; Cheng, Z. Experimental investigation on molecular-scale mechanism of wettability alteration induced by supercritical carbon dioxide-water-rock reaction. *J. Pet. Sci. Eng.* **2021**, *205*, 108798.
- (13) Wu, X.; Ning, Z.; Qi, R.; Wang, Q.; Huang, L. Pore characterization and inner adsorption mechanism investigation for

- methane in organic and inorganic matters of shale. *Energy Fuels* **2020**, *34*, 4106.
- (14) Huang, L.; Khoshnood, A.; Firoozabadi, A. Swelling of Kimmeridge kerogen by normal-alkanes, naphthenes and aromatics. *Fuel* **2020**, *267*, 117155.
  - (15) Wang, T.; Tian, S.; Li, G.; Sheng, M.; Ren, W.; Liu, Q.; Zhang, S. Molecular Simulation of CO<sub>2</sub>/CH<sub>4</sub> Competitive Adsorption on Shale Kerogen for CO<sub>2</sub> Sequestration and Enhanced Gas Recovery. *J. Phys. Chem. C* **2018**, *122*, 17009–17018.
  - (16) Lyu, C.; Ning, Z.; Chen, M.; Wang, Q. Experimental study of boundary condition effects on spontaneous imbibition in tight sandstones. *Fuel* **2019**, *235*, 374–383.
  - (17) Cheng, Z.; Ning, Z.; Yu, X.; Wang, Q.; Zhang, W. New insights into spontaneous imbibition in tight oil sandstones with NMR. *J. Pet. Sci. Eng.* **2019**, *179*, 455–464.
  - (18) Mohammed, M.; Babadagli, T. Wettability alteration: A comprehensive review of materials/methods and testing the selected ones on heavy-oil containing oil-wet systems. *Adv. Colloid Interface Sci.* **2015**, *220*, 54–77.
  - (19) Zhang, X.; Lin, B.; Yang, W.; Shen, C. Experimental study on the influence of energy conversion in the process of load coal plasma breakdown. *Energy* **2021**, *218*, 119469.
  - (20) Guo, J.; Kang, T.; Kang, J.; Chai, Z.; Zhao, G. Accelerating methane desorption in lump anthracite modified by electrochemical treatment. *Int. J. Coal Geol.* **2014**, *131*, 392–399.
  - (21) Yan, F.; Lin, B.; Zhu, C.; Zhou, Y.; Liu, X.; Guo, C.; Zou, Q. Experimental investigation on anthracite coal fragmentation by high-voltage electrical pulses in the air condition: Effect of breakdown voltage. *Fuel* **2016**, *183*, 583–592.
  - (22) Zhang, X.; Lin, B.; Li, Y.; Zhu, C.; Kong, J.; Li, Y. Enhancement effect of NaCl solution on pore structure of coal with high-voltage electrical pulse treatment. *Fuel* **2019**, *235*, 744–752.
  - (23) Guo, H.; Chen, C.; Liang, W.; Zhang, Y.; Duan, K.; Zhang, P. Enhanced biomethane production from anthracite by application of an electric field. *Int. J. Coal Geol.* **2020**, *219*, 103393.
  - (24) Ghosh, B.; Shalabi, E. W. A.; Haroun, M. The Effect of DC Electrical Potential on Enhancing Sandstone Reservoir Permeability and Oil Recovery. *Pet. Sci. Technol.* **2012**, *30*, 2148–2159.
  - (25) Ansari, A.; Haroun, M.; Rahman, M. M.; Chilingar, G. V. Electrokinetic driven low-concentration acid improved oil recovery in Abu Dhabi tight carbonate reservoirs. *Electrochim. Acta* **2015**, *181*, 255–270.
  - (26) Zhang, W.; Ning, Z.; Zhang, B.; Wang, Q.; Cheng, Z.; Huang, L.; Qi, R.; Shang, X. Experimental investigation of driving brine water for enhanced oil recovery in tight sandstones by DC voltage. *J. Pet. Sci. Eng.* **2019**, *180*, 485–494.
  - (27) Zhang, X.; Lin, B.; Zhu, C.; Yan, F.; Liu, T.; Li, Y. Petrophysical variation of coal treated by cyclic high-voltage electrical pulse for coalbed methane recovery. *J. Pet. Sci. Eng.* **2019**, *178*, 795–804.
  - (28) Yun, J.; Zhang, N. A discussion on the electrochemical recovery method and its mechanism. *Pet. Explor. Dev.* **1998**, *25*, 57–58.
  - (29) Kang, G.; Kang, T.; Guo, J.; Kang, J.; Zhang, R.; Zhang, X.; Zhao, G.; Zhang, B.; Li, L.; Zhang, L. Effect of electric potential gradient on methane adsorption and desorption behaviors in lean coal by electrochemical modification: implications for coalbed methane development of Dongqu mining, China. *ACS Omega* **2020**, *5*, 24073–24080.
  - (30) Zhang, X.; Lin, B.; Zhu, C.; Li, Y.; Yan, F. Experimental and numerical simulation analyses of selective fragmentation of coal samples by plasma. *Fuel* **2019**, *255*, 115717.
  - (31) Gao, Z.; Fan, Y.; Hu, Q.; Jiang, Z.; Cheng, Y.; Xuan, Q. A review of shale wettability characterization using spontaneous imbibition experiments. *Mar. Pet. Geol.* **2019**, *109*, 330–338.
  - (32) Li, S.; Liu, Y.; Xue, L.; Yang, L.; Yuan, Z. Experimental Investigation on the Pore-Scale Mechanism of Improved Sweep Efficiency by Low-Salinity Water Flooding Using a Reservoir-on-a-Chip. *ACS Omega* **2021**, *6*, 20984–20991.

- (33) Wang, H.; Zhang, L.; Wang, D.; He, X. Experimental investigation on the wettability of respirable coal dust based on infrared spectroscopy and contact angle analysis. *Adv. Powder Technol.* **2017**, *28*, 3130–3139.
- (34) Zhou, Y.; Albijanic, B.; Wang, Y.; Yang, J. Characterizing surface properties of oxidized coal using FTIR and contact angle measurements. *Energy Sources, Part A* **2018**, *40*, 1559–1564.
- (35) Arif, M.; Jones, F.; Barifcani, A.; Iglauer, S. Influence of surface chemistry on interfacial properties of low to high rank coal seams. *Fuel* **2017**, *194*, 211–221.
- (36) Zhou, G.; Xu, C.; Cheng, W.; Zhang, Q.; Nie, W. Effects of Oxygen Element and Oxygen-Containing Functional Groups on Surface Wettability of Coal Dust with Various Metamorphic Degrees Based on XPS Experiment. *J. Autom. Methods Manage. Chem.* **2015**, *2015*, 467242.
- (37) Tang, H.; Zhao, L.; Sun, W.; Hu, Y.; Han, H. Surface characteristics and wettability enhancement of respirable sintering dust by nonionic surfactant. *Colloids Surf., A* **2016**, *509*, 323–333.
- (38) Xia, W.; Niu, C.; Li, Y. Effect of heating process on the wettability of fine coals of various ranks. *Can. J. Chem. Eng.* **2017**, *95*, 475–478.
- (39) Xu, C.; Wang, D.; Wang, H.; Xin, H.; Ma, L.; Zhu, X.; Zhang, Y.; Wang, Q. Effects of chemical properties of coal dust on its wettability. *Powder Technol.* **2017**, *318*, 33–39.
- (40) Jingna, X.; Guanhua, N.; Hongchao, X.; Shang, L.; Qian, S.; Kai, D. The effect of adding surfactant to the treating acid on the chemical properties of an acid-treated coal. *Powder Technol.* **2019**, *356*, 263–272.
- (41) Guanhua, N.; Hongchao, X.; Shang, L.; Qian, S.; Dongmei, H.; Yanying, C.; Ning, W. The effect of anionic surfactant (SDS) on pore-fracture evolution of acidified coal and its significance for coalbed methane extraction. *Adv. Powder Technol.* **2019**, *30*, 940–951.
- (42) Guanhua, N.; Zhao, L.; Qian, S.; Shang, L.; Kai, D. Effects of [Bmim][Cl] ionic liquid with different concentrations on the functional groups and wettability of coal. *Adv. Powder Technol.* **2019**, *30*, 610–624.
- (43) Guanhua, N.; Qian, S.; Meng, X.; Hui, W.; Yuhang, X.; Weimin, C.; Gang, W. Effect of NaCl-SDS compound solution on the wettability and functional groups of coal. *Fuel* **2019**, *257*, 116077.
- (44) Sonibare, O. O.; Haeger, T.; Foley, S. F. Structural characterization of Nigerian coals by X-ray diffraction, Raman and FTIR spectroscopy. *Energy* **2010**, *35*, 5347–5353.
- (45) Song, Y.; Jiang, B.; Han, Y. Macromolecular response to tectonic deformation in low-rank tectonically deformed coals (TDCs). *Fuel* **2018**, *219*, 279–287.
- (46) Shi, Q.; Qin, B.; Bi, Q.; Qu, B. Changes in the Surface Structure of Coal Caused by Igneous Intrusions and Their Effect on the Wettability. *Energy Fuels* **2018**, *32*, 9371–9379.
- (47) Zhang, R.; Xing, Y.; Xia, Y.; Luo, J.; Tan, J.; Rong, G.; Gui, X. New insight into surface wetting of coal with varying coalification degree: An experimental and molecular dynamics simulation study. *Appl. Surf. Sci.* **2020**, *511*, 145610.
- (48) Yan, J.; Bai, Z.; Bai, J.; Guo, Z.; Li, W. Effects of organic solvent treatment on the chemical structure and pyrolysis reactivity of brown coal. *Fuel* **2014**, *128*, 39–45.
- (49) Li, Y.; Zong, Z.-M.; Zhang, Y.-Y.; Wei, X.-Y.; Zhu, Y. Thermal treatment of Shengli lignite and subsequent oxidation. *J. Anal. Appl. Pyrolysis* **2020**, *152*, 104810.
- (50) Huang, L.; Ning, Z.; Wang, Q.; Qi, R.; Li, J.; Zeng, Y.; Ye, H.; Qin, H. Thermodynamic and Structural Characterization of Bulk Organic Matter in Chinese Silurian Shale: Experimental and Molecular Modeling Studies. *Energy Fuels* **2017**, *31*, 4851–4865.
- (51) He, X.; Liu, X.; Nie, B.; Song, D. FTIR and Raman spectroscopy characterization of functional groups in various rank coals. *Fuel* **2017**, *206*, 555–563.
- (52) He, X.; Liu, X.; Song, D.; Nie, B. Effect of microstructure on electrical property of coal surface. *Appl. Surf. Sci.* **2019**, *483*, 713–720.
- (53) Zhao, J.; Deng, J.; Chen, L.; Wang, T.; Song, J.; Zhang, Y.; Shu, C.-M.; Zeng, Q. Correlation analysis of the functional groups and exothermic characteristics of bituminous coal molecules during high-temperature oxidation. *Energy* **2019**, *181*, 136–147.
- (54) Wang, J.; He, Y.; Li, H.; Yu, J.; Xie, W.; Wei, H. The molecular structure of Inner Mongolia lignite utilizing XRD, solid state <sup>13</sup>C NMR, HRTEM and XPS techniques. *Fuel* **2017**, *203*, 764–773.
- (55) Liu, X.; Song, D.; He, X.; Nie, B.; Wang, L. Insight into the macromolecular structural differences between hard coal and deformed soft coal. *Fuel* **2019**, *245*, 188–197.
- (56) Zhang, L.; Hu, S.; Chen, Q.; Xiao, L.; Syed-Hassan, S. S. A.; Jiang, L.; Wang, Y.; Su, S.; Xiang, J. Molecular structure characterization of the tetrahydrofuran-microwave-extracted portions from three Chinese low-rank coals. *Fuel* **2017**, *189*, 178–185.
- (57) Han, W.; Zhou, G.; Zhang, Q.; Pan, H.; Liu, D. Experimental study on modification of physicochemical characteristics of acidified coal by surfactants and ionic liquids. *Fuel* **2020**, *266*, 116966.
- (58) Ge, L.; Zhang, Y.; Xu, C.; Wang, Z.; Zhou, J.; Cen, K. Influence of the hydrothermal dewatering on the combustion characteristics of Chinese low-rank coals. *Appl. Therm. Eng.* **2015**, *90*, 174–181.
- (59) Hongchao, X.; Guanhua, N.; Jingna, X.; Weimin, C.; Meng, X.; Yuhang, X.; Hui, W.; Gang, W. The effect of SDS synergistic composite acidification on the chemical structure and wetting characteristics of coal. *Powder Technol.* **2020**, *367*, 253.
- (60) Yin, B.; Kang, T.; Kang, J.; Chen, Y. Experimental and mechanistic research on enhancing the strength and deformation characteristics of fly-ash-cemented filling materials modified by electrochemical treatment. *Energy Fuels* **2018**, *32*, 3614–3626.
- (61) Dey, S. Enhancement in hydrophobicity of low rank coal by surfactants - A critical overview. *Fuel Process. Technol.* **2012**, *94*, 151–158.
- (62) Lin, X.; Wang, C.; Ideta, K.; Miyawaki, J.; Nishiyama, Y.; Wang, Y.; Yoon, S.; Mochida, I. Insights into the functional group transformation of a chinese brown coal during slow pyrolysis by combining various experiments. *Fuel* **2014**, *118*, 257–264.
- (63) Xi, X.; Jiang, S.; Zhang, W.; Wang, K.; Shao, H.; Wu, Z. An experimental study on the effect of ionic liquids on the structure and wetting characteristics of coal. *Fuel* **2019**, *244*, 176–183.
- (64) Niu, Z.; Liu, G.; Yin, H.; Zhou, C. Devolatilization behaviour and pyrolysis kinetics of coking coal based on the evolution of functional groups. *J. Anal. Appl. Pyrolysis* **2018**, *134*, 351–361.
- (65) Niu, Z.; Liu, G.; Yin, H.; Zhou, C.; Wu, D.; Yousaf, B.; Wang, C. In-situ FTIR study of reaction mechanism and chemical kinetics of a Xundian lignite during non-isothermal low temperature pyrolysis. *Energy Convers. Manage.* **2016**, *124*, 180–188.
- (66) Tahmasebi, A.; Yu, J.; Han, Y.; Li, X. A study of chemical structure changes of Chinese lignite during fluidized-bed drying in nitrogen and air. *Fuel Process. Technol.* **2012**, *101*, 85–93.
- (67) Niu, Z.; Liu, G.; Yin, H.; Wu, D.; Zhou, C. Investigation of mechanism and kinetics of non-isothermal low temperature pyrolysis of perhydrous bituminous coal by in-situ FTIR. *Fuel* **2016**, *172*, 1–10.
- (68) Mursito, A. T.; Hirajima, T.; Listiyowati, L. N.; Sudarsono, S. Surface physicochemical properties of semi-anthracitic coal from Painan-Sumatra during air oxidation. *Int. J. Coal Sci. Technol.* **2018**, *5*, 156–166.
- (69) Wang, D.; Zhong, X.; Gu, J.; Qi, X. Changes in active functional groups during low-temperature oxidation of coal. *Min. Sci. Technol.* **2010**, *20*, 35–40.
- (70) Li, Q.-W.; Xiao, Y.; Zhong, K.-Q.; Shu, C.-M.; Lü, H.-F.; Deng, J.; Wu, S. Overview of commonly used materials for coal spontaneous combustion prevention. *Fuel* **2020**, *275*, 117981.
- (71) Wang, D.; Kang, T.; Han, W.; Liu, Z. Electrochemical modification of tensile strength and pore structure in mudstone. *Int. J. Rock Mech. Min. Sci.* **2011**, *48*, 687–692.
- (72) Zhang, W.; Ning, Z.; Wang, B. Experimental investigation of the variations in the pore structure of tight sandstones subjected to an electric field. *J. Pet. Sci. Eng.* **2021**, *204*, 108690.
- (73) Xin, H.; Wang, H.; Kang, W.; Di, C.; Qi, X.; Zhong, X.; Wang, D.; Liu, F. The reburning thermal characteristics of residual structure of lignite pyrolysis. *Fuel* **2020**, *259*, 116226.

(74) Qiu, S.; Zhang, S.; Zhou, X.; Zhang, Q.; Qiu, G.; Hu, M.; You, Z.; Wen, L.; Bai, C. Thermal behavior and organic functional structure of poplar-fat coal blends during co-pyrolysis. *Renewable Energy* **2019**, *136*, 308–316.

(75) Liu, P.; Wang, L.; Zhou, Y.; Pan, T.; Lu, X.; Zhang, D. Effect of hydrothermal treatment on the structure and pyrolysis product distribution of Xiaolongtan lignite. *Fuel* **2016**, *164*, 110–118.